

Heterophase polymerization: pressures, polymers, particles

Kathleen Krüger · Chunxiang Wei · Sukanya Nuasaen ·
Patrick Höhne · Pramuan Tangboriboonrat · Klaus Tauer

Received: 18 July 2014 / Revised: 27 October 2014 / Accepted: 29 October 2014 / Published online: 27 November 2014
© Springer-Verlag Berlin Heidelberg 2014

Abstract Following the swelling of single-polymer beads and the polymerization of single-monomer droplets are unconventional methods to study heterophase polymerizations. However, the focus on the behavior of single-colloidal entities allowed surprisingly a degree of abstraction which was unattainable so far with conventional investigation strategies. The experimental results revealed an unexpected behavior of polymerizing droplets and led to the discovery of the importance of the swelling pressure for any kind of heterophase polymerization process. The action of the swelling pressure is independent of any special design of the process and only requires the coexistence of monomer and polymer in confined reaction volumes.

Keywords Single droplet polymerization · Heterophase polymerization · Swelling pressure · Latex particle formation

Introduction

Pressure plays a decisive role in all heterophase polymerizations in which colloidal dimensions are involved. More precisely, several pressures must be considered which are the pressure of the gas phase (P_G) or the overall pressure in the reactor, the Laplace pressure inside the colloidal entities (P_L),

and the swelling pressure generated inside the polymerizing particles (P_S). P_G can be deliberately chosen by the experimenter and controls both the composition of the gas phase and the amount of gas phase dissolved in the continuous phase which is mainly important for gaseous monomers. P_L depends inversely on the size of the colloidal objects (droplets and particles) and particularly determines the stability of the smaller droplets. P_S influences the amount of monomer inside the particles and hence also the rate of polymerization.

Considering the centennial history of heterophase polymerization (HP), it is quite astonishing that a comprehensive treatment of how P_G , P_L , and P_S concertedly determine the polymerization scene is missing.

We want to fill this gap and discuss the interrelation of P_G , P_L , and P_S as well as their influence on HP on the base of experimental data backed up by thermodynamic considerations. Because these pressures influence not only heterophase polymerization in general but also certain aspects in very specific ways, we necessarily had to combine very different experimental results in one script. In order to ease the discussion, we will consider cases where the assumption of a heterogeneous system prior to polymerization is undisputed. Under such condition, starting with a monomer emulsion and ending with a polymer dispersion, HP can be essentially described as transition between different colloidal states controlled by polymerization. The key issue in this context is the role of monomer droplets, and hence, we are presenting mainly, but not exclusively, experimental data where the initiation of the polymerization takes place inside the monomer droplets. To study the role of monomer droplets, we developed an experimental procedure to follow the behavior of a single polymerizing droplet. However, it was exactly this rather strange experimental approach to study heterophase polymerization, where under technical conditions, typically, a myriad of droplets participate in the reaction, which allowed us to get surprising experimental results and new insights.

Electronic supplementary material The online version of this article (doi:10.1007/s00396-014-3448-9) contains supplementary material, which is available to authorized users.

K. Krüger · C. Wei · S. Nuasaen · P. Höhne · K. Tauer (✉)
Max Planck Institute of Colloids and Interfaces, D-14424 Potsdam,
Germany
e-mail: klaus.tauer@mpikg.mpg.de

S. Nuasaen · P. Tangboriboonrat
Department of Chemistry, Faculty of Science, Mahidol University,
Rama 6 Road, Phayathai, Bangkok 10400, Thailand

We are discussing the influence of pressure effects on colloidal heterophase polymerizations which can be controlled by the experimenter to different degrees. The gas phase pressure can be controlled to a great extent, the swelling pressure less, and the Laplace pressure the least. To get deeper knowledge about the interrelation between these pressures on the one hand and with the polymerization kinetics on the other hand is important for better understanding the mechanism of heterophase polymerizations.

Experimental information

Hydrophobically initiated emulsion polymerization

Materials

Styrene (99 % purity, Sigma-Aldrich) was distilled in darkness under reduced pressure (14 mbar, 40 °C) to remove inhibitors and stored in a refrigerator before use. Sodium dodecyl sulfate (SDS) (purity ≥ 99 % for electrophoresis, ROTH) and bis-(2,4,6-trimethylbenzoyl-phenylphosphine oxide) (Irgacure 819) (Ciba Specialty Chemicals) were used as received.

Polymerization

All photoinitiated polymerizations were carried out at 25 °C between two standard fluorescent tubes (Osram L 18 W, light color 840, Lumilux, cool white); for details, see [1, 2] in borosilicate glass vials with Rotaflor[®] stopcock with a Teflon-coated magnetic stirring bar at a stirring rate of 500 rpm. The standard recipe for the emulsion polymerization was as follows: 20 g of water, 4.5 g of styrene, 0.6 g of SDS, and 0.02 g of initiator (0.048 mmol). If not otherwise stated, the polymerization time was fixed to 20 h.

The reaction mixtures for the hydrophobically initiated emulsion polymerization (HIEP) were degassed, and the glass vials were placed in the middle between two fluorescent tubes on a multipoint magnetic stirrer plate. At the end of the polymerization after a predetermined reaction time, the vials were removed from the light source and the coagulum was separated from the latex by filtration through glass frits of pore size 1.

The polymerization data presented here were reproduced several times so that the discussed effects are statistically secured.

Anisotropic particles

Synthesis of polystyrene seed particles

Polystyrene (PS) latex particles were synthesized by the soap-free emulsion polymerization. DI water (190 g) was bubbled with nitrogen gas for 30 min before adding styrene monomer

(20 g). The polymerization was started with the addition of ammonium peroxydisulfate (APS) solution (0.2 g in 10 g of water) at 70 °C and carried out for 22 h. The residual monomers, electrolyte, and water-soluble oligomers were removed by centrifugation (10,000 rpm, 20 min) and washed thrice with DI water. The linear PS particles were further used as seed in the preparation of cross-linked PS seed.

Synthesis of cross-linked polystyrene seed particles

Of linear PS seed particles, 5.0 mL (20 % w/v) dispersed in a 1 % w/v poly(vinyl alcohol) (PVAI) aqueous solution was mixed with a 20 vol.% monomer emulsion which was made in a 1 % w/v PVAI aqueous solution by homogenizing at 8000 rpm for 1 min. The monomer solution consisted of styrene (St), divinylbenzene (DVB), and 2, 2'-azobis (2,4-dimethylvaleronitrile) (V-65) initiator (0.5 wt.%). To study the effect of seed cross-link density on final anisotropic morphology, DVB was varied from 0, 1, and 5 to 10 vol.% based on total monomer. The volume ratio of the monomer solution to the seed particles was 4:1. The mixture was swollen with PS seed particles at RT for 20 h. Consequently, Frey's salt (10^{-4} mol/L) was added and polymerization was performed at 70 °C for 8 h in an oil bath.

Preparation of anisotropic particles

Anisotropic (ANI) particles were synthesized via the seeded polymerization with cross-linked polystyrene (CPS) seed particles [3]. A 20 % w/v CPS dispersion (5.0 mL) was prepared in a 1 % w/v PVAI aqueous solution. A 20 vol.% monomer emulsion which composed of MMA and V-65 initiator (0.5 wt.%) was homogenized in a 1 % w/v PVAI aqueous at 8000 rpm for 1 min, and then mixed with CPS dispersion. In this case, the volume ratio of the monomer solution to the CPS particles was 4:1. The mixture was swollen with CPS seed particles at RT for 20 h. Thereafter, Frey's salt (10^{-4} mol/L) was charged before the seeded polymerization at 70 °C for 8 h. The anisotropic composite particles were cleaned by sedimentation and washed thrice with DI water.

Identification of anisotropic phase

ANI particles were dispersed in glacial acetic acid (g-AA) (1 mg/mL) which was a selective solvent for poly (methyl methacrylate) (PMMA) at room temperature for 24 h. The dispersed ANI particles were allowed to sediment for 24 h; dissolved and undissolved components were separated. Dissolved components were then characterized using SEC and ATR-FTIR. Undissolved components were washed, dried, and characterized.

Observation of polymerizing droplets

A digital microscope (Keyence VHX with VH-Z100 objective) was used in dual function to start the photopolymerization with the microscope light and to monitor the polymerizing droplets. A particular advantage of the Keyence microscope is the long distance between object and objective which allows the observation inside cuvettes in combination with changing the illumination angle. The latter features allows to the observation of scattered light even from objects whose size is below the detection limit of optical microscopy. All experiments were carried out in closed optical cuvettes at ambient conditions without stirring. The droplets were generated by shaking the cuvettes gently. Then, the cuvette was placed in the holder (cf. Fig. 6) and the objective focused on a region in the aqueous phase where suited droplets were spotted. Snapshots were taken at predetermined time intervals and automatically stored. The cuvette was filled with 1 mL of organic phase (pure styrene or styrene plus 10 wt.% DVB, or pure DVB, or ethyl benzene) and 2 mL of water. If applied, the Irgacure819 amount was 4.5 mg dissolved in 1 mL of the organic phase. Some experiments were carried out with 20 mg of SDS dissolved in 2 mL of water.

Polymerization with poly(vinyl alcohol) stabilizer

Poly(vinyl alcohol) (PVAL, type M05/140 with 86–89 mol% OH groups) a gift from Wacker-Chemie was used as received. Potassium peroxydisulfate (KPS) and 2,2'-azobis(2-methylpropionamide) dihydrochloride (V-50) both from Sigma-Aldrich, dibenzoyl peroxide (BPO), 2,2'-azobis(2,4-dimethyl valeronitrile) (V-65), 2,2'-azobis[2-methyl-*N*-(2-hydroxyethyl) propionamide] (VA-086), and 4,4'-azobis(4-cyanopentanoic acid) (V-501), all from Wako, were used as received.

The oil-soluble initiators were dissolved in styrene monomer (0.01 g of each in 2 mL) before the addition of 8 mL aqueous solution of PVAL (1 wt.% PVAL). The water-soluble initiators were dissolved in the PVAL solution before addition of 2 mL of styrene. Emulsification was carried out at 8000 rpm for 1 min with an ultra turrax mixer (T25, Jahnke and Kunkel) before the 25-mL glass vial was closed with a rubber stopper and the mixture deaerated by purging nitrogen via two syringe needles for 20 min while magnetically stirred. Then, the vials were placed in an oil bath at the reaction temperature of 70 °C on a heatable magnetic stirrer plate (400 rpm) for 7 h.

For the photoinitiated polymerizations with Irgacure819 with and without PVAL as stabilizer, 0.02 g of initiator was dissolved in 4.5 g styrene. Then, the monomer-initiator solution was mixed with either 20 mL of water or 20 mL aqueous PVAL solution (1 wt.%) T in 25-mL glass vial (magnetic stirring 400 rpm) sealed with rubber stopper and degassed for 20 min by purging nitrogen through two syringe needles. The polymerization was conducted at room temperature by

placing the glass vials between two standard fluorescent tubes (Osram L 18 W, light color 840, Lumilux, cool white) for 20 h.

Characterization

The solids content (FG) was determined with a HR 73 halogen moisture analyzer (Mettler Toledo, Giessen). With FG, the monomer conversion to latex (X_L) is calculated as described in [1, 2]. X_L is a measure only of the amount of monomer converted into latex and does not consider the amount of polymer that is present in the reaction mixture as coagulum. Coagulum is the entire polymer that does not pass through the glass frit of pore size 1.

The intensity-weighted average particle size (D) was measured by dynamic light scattering with NICOMP particle sizer (model 380 PSS, Santa Barbara, California). Molecular weight distributions (MWD) were determined by size exclusion chromatography (SEC) on the basis of polystyrene standards (PSS; Mainz). For experimental details, see [1, 2].

Scanning electron microscopy (SEM) was performed according to standard procedures with a high-resolution scanning electron microscope operating at an acceleration voltage of 3 kV (LEO1550 Gemini, Carl Zeiss AG, Germany).

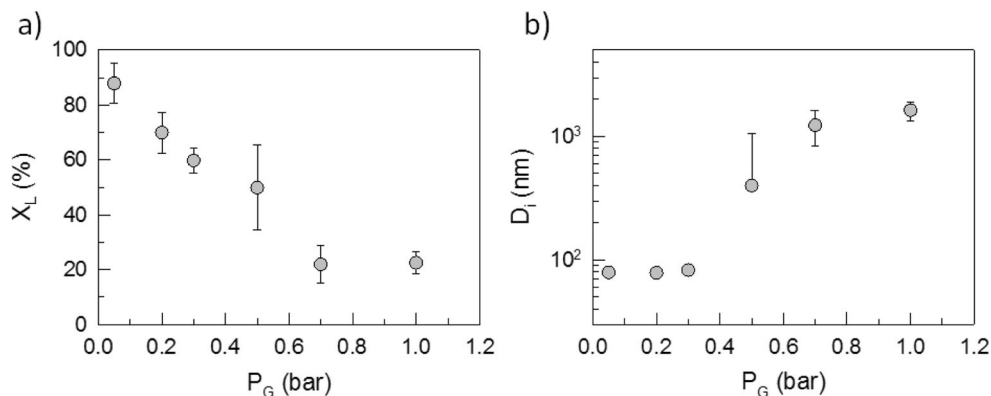
Experimental results

Gas phase pressure

Recently, we reported the influence of the composition of the gas phase on the kinetics of a special variant of heterophase polymerization for which we coined the name hydrophobically initiated emulsion polymerization (HIEP) [1, 2, 4]. The characteristic feature of HIEP is a kind of mishmash between emulsion and suspension polymerization that is the use of a typically emulsion polymerization stabilizer such as sodium dodecyl sulfate in combination with an initiation reaction which is confined inside the monomer droplets. This strict requirement is realized by using either initiator-free initiation mechanisms such as photo-initiation and thermal self-initiation or extremely hydrophobic initiators. In order to avoid thermal mixing effects and side reactions, we carried out polymerization at ambient temperature with Irgacure 819 as very efficient photoinitiator with solubility in water $<10^{-7}$ M [5] which might be considered in comparison with styrene as super-hydrophobic. However, as discussed below, the choice of the initiation system basically has no effect on the experimental results.

In HIEP, different kinetic scenarios take place in parallel in dependence on the droplet size which already has been discussed [4]. Provided the droplets are stable, then the final particle size distribution (PSD) should somehow reflect the initial droplet size distribution (DSD). However, this quite

Fig. 1 Correlation between gas phase (air) pressure (P_G) and latex conversion (graph **a**) and average latex particle size (graph **b**) for HIEP of styrene after polymerization time of 20 h



straightforward assumption is possibly too simple because the experimental data show that both the portion of emulsion and suspension polymerization products and the resulting PSD changes drastically in dependence on the gas phase composition, under otherwise identical conditions [1].

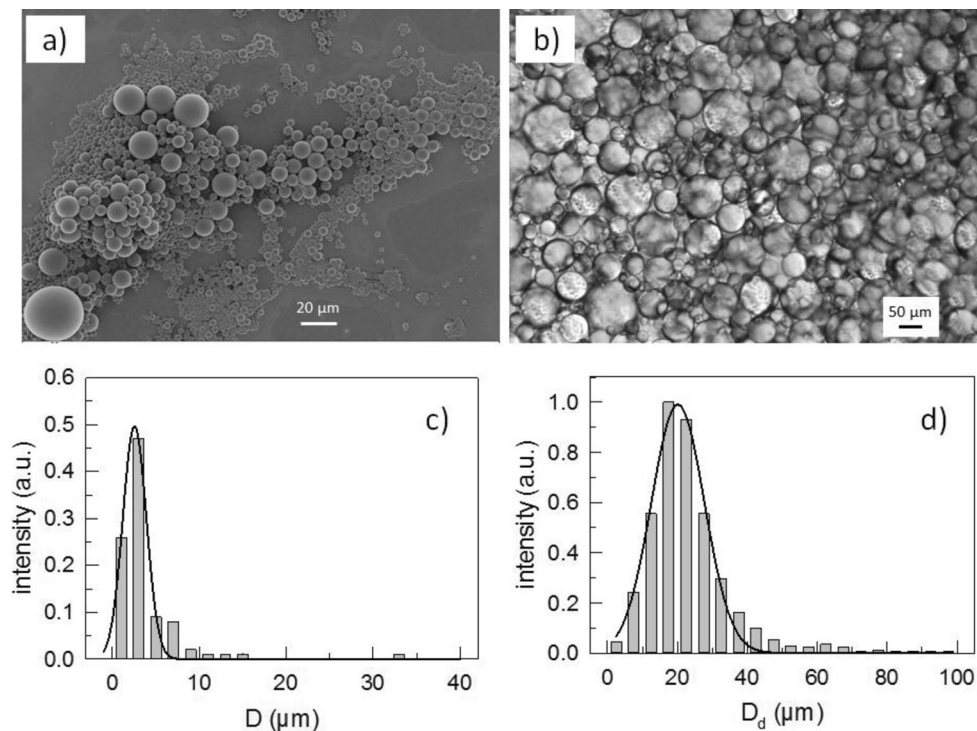
Here, we report experimental results showing the strong influence of P_G on styrene HIEP. The data depicted in Fig. 1 reveal that with increasing gas phase pressure (here air) the latex conversion decreases and the average particle size increases. Decreasing latex conversion indicates that the portion of emulsion polymerization is reduced which leads eventually to a drop in the overall rate of polymerization (cf. discussion in [4]).

The comparison of the droplet and the particle size distribution for the polymerization at $P_G=0.7$ bar (Fig. 2) with quite a high portion of suspension polymerization shows a shift of the maximum by about a factor of ten towards lower sizes.

Even considering the lower overall conversion at this air pressure and the size-dependent polymerization rate due to the “negative segregation effect” as discussed in [4] cannot solely explain this shift.

Clearly, there is a certain influence of the increasing oxygen content on the rate of polymerization particularly for initiation in the droplets due to the higher solubility of air in organic solvents than in water [6]. However, this kinetically restricted view does not explain the enormous difference in the average particle size by more than a factor of ten and the increasing portion of emulsion polymerization in the overall kinetics with decreasing pressure. In other words, it is not possible only with the inhibition effect of air to explain the experimentally observed inverse relation between latex conversion and average particle size (mentally combining graph “a” and “b” of Fig. 1).

Fig. 2 Comparison of droplet size distribution (light microscopy image **b** and graph **d**) and latex particle size distribution (SEM micrograph **a** and graph **c**) for polymerization at gas phase pressure $P_G=0.7$ bar; the *lines* are Gauss fits of the histograms obtained from enumerating the corresponding images with average $2.5 \mu\text{m}$ and standard deviation $1.4 \mu\text{m}$ for graph **c** and average $20.1 \mu\text{m}$ and standard deviation $7.6 \mu\text{m}$ for graph **d**; number of counted particles are 100 and 830 for the particles (graph **c**) and the droplets (graph **d**), respectively



Swelling of polymer particles

Swelling is particularly important when the formation of latex particles takes place outside the monomer phase as typically considered to be the case in classical emulsion polymerization. In this case, it is assumed since Harkins that the role of the monomer drops is “to act as a storehouse of monomer from which its molecules diffuse into the aqueous phase and from this into either soap micelles or polymer monomer latex particles” [7]. This point of view has not much changed over the decades. Also, in recent texts on emulsion polymerization kinetics, the question how the monomer enters the particles plays rather an inferior role. The comforting assumption is that it is just there, where it is expected to be—in the monomer swollen latex particles. Exemplarily, “Interval 2 is characterised by a constant number of particles (the polymerisation locus) and the presence of monomer droplets. The monomer-swollen particles grow and the monomer concentration within these particles is kept constant by monomer diffusing through the water phase from the monomer droplets” [8].

Frequently, the Morton-Kaizerman-Altier equation [9] is used as thermodynamic justification to swelling and for statements of the kind as given above. However, experimental evidence has been presented that both the MKA equation is not complete [10, 11] and the assumption of homogeneously swollen particles may not be the typical case under polymerization conditions (cf. below and discussion in [12]).

If we consider styrene polymerization the growth of an average chain, even assuming quite a high degree of polymerization of 10^4 takes place in less than a minute. According to the above statement, the corresponding amount of monomer should be replaced within this period of time. Interestingly, if swelling of latex particles is studied [9, 10] or if swelling is necessary as separate step during the synthesis of special latex particles [3, 13–17], the time for which swelling is allowed is typically in the order of 24 h. The clear experimental control whether this time is sufficient or too long or too short is quite challenging for particles with colloidal dimensions. The same holds, of course on a different time scale, for the question whether the monomer consumed during the characteristic propagation time can be replaced by fresh monomer in the entire particle volume more or less instantaneously. In order to approach the issue and to illustrate the problem, we carried out the kind of model experiments (cf. Fig. 3) with polystyrene beads under the two extreme conditions of “swelling” in a pure solvent (S1) and when a water layer separates the bead from the solvent (S2). For the visual observation and the sake of illustration only, polystyrene beads have been used with a diameter of about 2 mm and instead of styrene as swelling agent a solvent with equally good solvency was used (either toluene or ethyl benzene). The behavior of the bead in pure solvent was investigated in two variants. In the first set of experiments, the bead was allowed to freely move in the pool

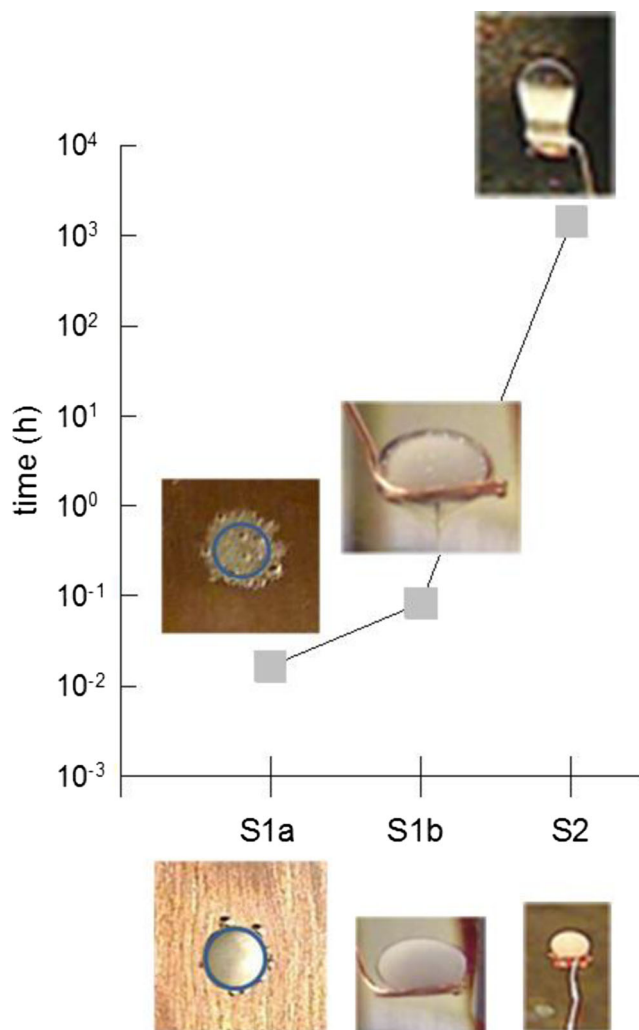


Fig. 3 Illustration of the swelling behavior of polystyrene beads (size about 2 mm) under different conditions with respect to the contact with swelling agent; the images below the *x*-axis show the bead immediately after insertion in the setup and the images above at the time as indicated by the squares in the graph; *S1a*, bead can freely move in a pool of toluene; *S1b*, bead is fixed in place in a pool of toluene; *S2*, bead is fixed in place in a pool of water (containing SDS at concentration above the critical micelle concentration) at a position about 1 cm below an ethyl benzene layer; the *circle* in the images for *S1a* indicates the changes within 1 min

of the solvent (*S1a*) whereas it was fixed in place in the second variant (*S1b*). For studying the interaction of the bead with the solvent in the presence of a separating water layer, the bead was fixed in place in the water phase.

Despite the fact that these swelling experiments are only a very rough approximation to the situation during heterophase polymerization, they nevertheless lead to interesting conclusions. Firstly, the direct contact between pure swelling agent and the polymer accelerates swelling enormously. The highly swollen state for the PS bead as depicted in Fig. 3 is observed for *S1a* after 1 min, for *S1b* after 5 min, and for *S2* after 1416 h (or 59 days) of swelling time. Secondly, the constant supply of pure swelling agent to the particle is another important

prerequisite for as fast as possible swelling. Comparing S1a and S1b shows that the freely moving bead which permanently seeks the contact with pure solvent (following the greatest difference in the chemical potential of the swelling agent) dissolves or decomposes much faster than the resting bead. The bead under condition S1a shows already after 1 min a uniform increase of the transparency over the entire volume and the interface has changed from smooth to very bumpy. Contrary, the bead fixed in place (S1b) is surrounded by an almost stagnant layer of polymer solution which prevents rapid penetration of swelling agent into the whole volume. The formation of the polymer solution shell is clearly to be seen (Fig. 3).

Thirdly, if the direct contact between the swelling agent and the polymer bead is held up by water, the uptake is drastically hindered. A visual change of the bead can be detected only after several days. The image of S2 shown in Fig. 3 depicts the highly swollen bead a few hours before liftoff into the ethyl benzene phase.

An interesting detail revealed by these experiments relates to the formation of gas bubbles which were observed only in S1a and S1b but not in S2. In our understanding, this is reasonable because the gas concentration in the organic phase is about an order of magnitude higher than in water [6] and the exothermic heat effect connected with swelling of polystyrene beads in toluene [18] causing bubble nucleation triggered by the interface. This is no surprise, but nothing else than classical heterogeneous nucleation in colloid chemistry [19].

The reason for the enormous difference between swelling according to S1 and S2 is besides the difference in the chemical potential of the swelling agent in both phases (here, one has to consider the chemical potential in the continuous phase and inside the bead) the swelling pressure acting in the latter case (cf. discussion below).

Anisotropic particles

The swelling pressure can also be used as a synthetic tool for the fabrication of non-spherical anisotropic polymer particles [3, 13–16]. This is typically a multistep synthesis starting with ordinary polystyrene particles which are used as seed in a second polymerization of a styrene divinylbenzene (DVB) mixture. Ideally, this seeded polymerization should lead to spherical particles where the linear polystyrene chains of the seed homogeneously interpenetrate the poly(styrene-DVB) network formed during the second polymerization. Then, we used these spherical semi-interpenetrating network particles as seed in a third polymerization of methyl methacrylate (MMA). During swelling and polymerization, an elastic stress is built up which is relaxed via budding on a weak region of the seed particles' interface. The stress relaxation occurs obviously quite fast, so that the formation of bulges takes place predominantly only in one direction starting from just a single, namely, the weakest spot of the swollen particles during polymerization. Simultaneous relaxation and

subsequent growth in two or three directions can happen, however, with much lower probability. These bulges are the loci where most of the second-stage monomer polymerizes and they keep in contact with the parental seed particles predominantly via chain entanglements. This scenario is basically confirmed by the sequence of SEM micrographs put together in Fig. SI-1.

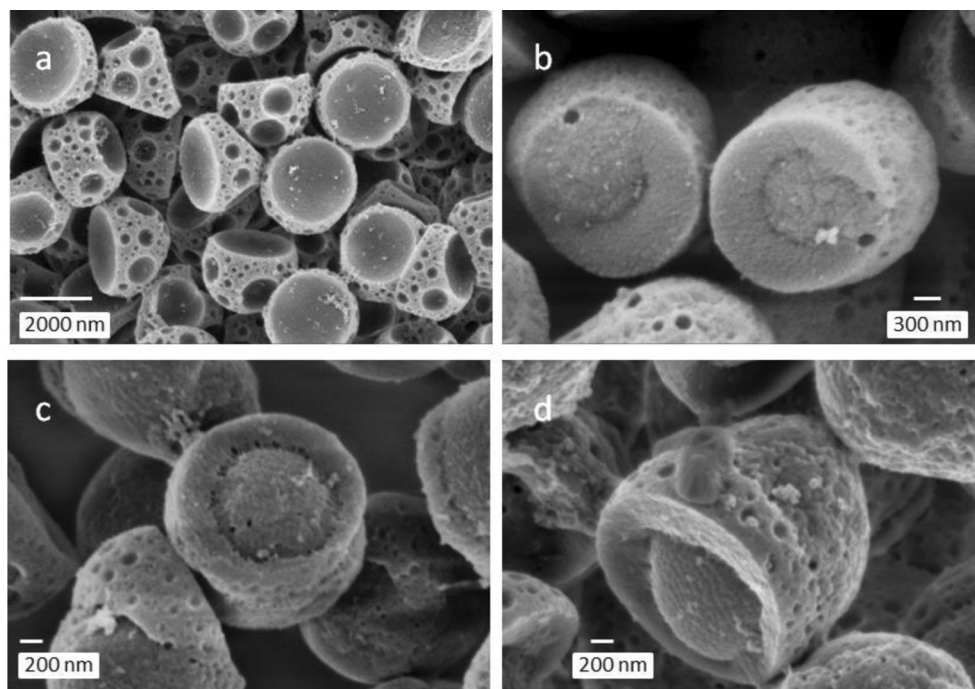
The SEM micrographs of Fig. SI-1 confirm that cross-linking of the seed particles is crucial for the development of an anisotropic shape. The final particles prepared with the uncross-linked seed are almost spherical (micrograph a of Fig. SI-1). Already, 1 vol% of DVB in the monomer mixture during the second-stage polymerization triggers the change to an ellipsoidal shape. These particles (micrograph b of Fig. SI-1) appear as if they were composed of two equally sized compartments. Increasing cross-linking density causes deviations from the homogeneous ellipsoidal shape with respect to both size and alignment of the compartments.

However, the exchange of the aqueous continuous phase with glacial acetic acid (g-AA) which is a selective solvent for PMMA causes a drastic change in the morphology of the remaining particles (Fig. 4) compared with both the final anisotropic and the seed particles after the second- and third-stage polymerization, respectively.

The treatment with g-AA removes practically only PMMA from the composite particles as proven by FT-IR spectroscopy (data not shown). During the contact with g-AA the PS remains in the glassy state, and hence, the depicted morphology (Fig. 4) is the result of the pressure and/or stress acting during the swelling with MMA and the third-stage polymerization. Following the principle of least constraint, the seed particles deform. Despite the fact that MMA is a solvent for PS, both polymers are not compatible and try to phase-separate during the polymerization which additionally contributes to the development of the final morphology of the composite particles.

Comparing the micrographs of the PS seed particles (right hand side of the micrographs a–d of Fig. SI-1) with the PS-residual-cores (PS-RCs) put together in Fig. 4 illustrates quite impressively the consequences of the total pressure or stress acting on them during swelling and polymerization. Interestingly, the micrograph of the uncross-linked PS-RC (micrograph a of Fig. 4) also shows strongly deformed structures though one might think that in these seed particles the pressure acts isotropically. In addition, these PS-RCs show many indentations (the darker regions) without any recognizable internal structures. These smooth regions are obviously the spots where PMMA domains were anchored in the PS cores. Remarkably, the uncross-linked PS-RCs possess each at least two quite large of such areas. Since the corresponding composite particles are spherical (left hand side of micrograph a of Fig. SI-1), the conclusion is straightforward that a PMMA shell with variable thickness surrounds the PS cores. The formation of an outer PMMA shell is driven by the tendency to decrease the interfacial energy to the continuous water phase [20].

Fig. 4 SEM micrographs illustrating the morphological features of the PS residual cores after removal of the PMMA from the composite particles; **a** without cross-linker, **b** 1, **c** 5, and **d** 10 % DVB in the monomer mixture; the bars indicate **a** 2 μm , **b** 300 nm, **c**, **d** 200 nm



However, the cross-linked PS-RCs show a significantly different morphology (micrographs “b–d” of Fig. 4). Firstly, the shape is elongated thus reflecting the original composite PS-PMMA particles. Secondly, all PS-RCs exhibit just a single huge spot where the main part of the PMMA was attached. The rest of the surface shows quite many but smaller indentations, compared with the uncross-linked PS-RCs. Obviously, the whole surface of these composite particles is also PMMA in order to minimize the excess free interaction energy with water. Thirdly and most amazingly, the PS-RCs clearly show core-shell morphology for all cross-linking densities. This is an important result because it contradicts homogenous swelling. In other words, it is not consistent with the assumption that after the swelling step, the swollen particles possess a radially homogeneous composition which would be drops of a styrene–DVB mixture containing dissolved PS. The polymerization of the styrene–DVB mixture should under such conditions lead to a semi-interpenetrating network exhibiting somehow homogeneous morphology but surely not such clear core-shell structure independent of the cross-linker content. This result is much more in accordance with a gradient structure of the swollen particles similar to that as depicted in Fig. 3 for the case S1b.

Observation of polymerizing droplets

The idea of controlling the final properties of polymer particles by designing properly the size and composition of the monomer droplets is fascinating but remained to this day, at least for aqueous heterophase polymerization, an unattainable dream. It is a common procedure to evaluate heterophase

polymerizations by considering the average properties of myriads of particles because only in this way, it is possible to determine overall monomer conversion and molecular weight distribution. In contrast, particularly, optical microscopy allows quite easily the observation of single droplets during the polymerization process. Of course, to draw meaningful conclusions, the observation of many different droplets is necessary, but this is quite a tedious undertaking. Nevertheless, we believe that such experiments are of significant relevance for studies of the mechanism of heterophase polymerization. Only the observation of an individual polymerizing droplet allows the direct study of its behavior whereas tracking a particular droplet in a real heterophase polymerization is practically impossible.

Images a and c of Fig. SI-2 elucidate the procedure employed in this study. Figure SI-2a shows a cuvette before (C_0) and after (C_f) the polymerization and Fig. SI-2c the cuvette (C_p) placed in the holder in front of the objective (o), illuminated from behind. The image b of Fig. SI-2 illustrates typical behavior of individual droplets before (subscript 0) and after few hours polymerization time (subscript t) for three different recipes (subscript 1–3). Despite all problems with such a procedure, the results we obtained so far are extremely promising and revealed unexpected and completely surprising behavior of polymerizing droplets. The objection that this optical method allows only the observation of droplets beyond a certain size is correct but not relevant and was already refuted by Galileo Galilei [21]. This “principle of similitude” as stated by R. C. Tolman “The fundamental entities of which the physical universe is constructed are of such a nature that from them a miniature universe could be constructed exactly

similar in every respect to the present universe.” allows the conclusion that the experimental observations discussed below very likely hold for much smaller droplets as well which, however, cannot be observed with optical microscopy [22, 23].

Considering the increase in density from styrene to polystyrene and assuming the droplet stays unchanged without any interaction (neither delivering nor uptake of monomer to or from the environment, respectively), the so isolated droplet must shrink during the polymerization in dependence on the monomer conversion X . Taking $d_m=0.9$ and $d_p=1.05$ g/cm³ as the monomer and polymer density at room temperature, respectively, the diameter of the drop should decrease at complete conversion to 0.95 of its initial size.

The images $b_{1,t}$ – $b_{3,t}$ of Figure SI-2 illustrate exemplarily some spectacular observations which are both moderate (b_2) and drastic decrease in size (b_3), increase in size (b_1), corona formation around the drops (b_1), and increasing turbidity of the continuous phase due to formation of highly mobile fine particles (b_1 – b_3 , and image c_f). The increasing turbidity causes blurring of the droplets and clearly indicates ongoing polymerization also in the continuous phase. It should be noted that this effect resembles the quite old problem of “emulsion particle formation in suspension polymerization,” an also industrially frequently occurring unwanted issue. Also, it is necessary to point out that polymerization takes place in the bulky monomer phase on top of the water leading to a high viscous PS in styrene solution or at longer polymerization times to glassy PS phase.

The duration of the polymerization is highly variable, but this is not considered to be critical. Typically, the behavior of the drop was recorded as long as changes could have been detected. The longest period of observation with continual changes lasted about 20 days (cf. Fig. 5) during which periods with only minimal variations alternate with sudden changes in shape and size. After about 20 days (exactly 479 h and 38 min), the last image (f of Fig. 5) shows compared with the initial droplet (image a) many small satellite particles surrounding the parental drop which, however, grew in size by the factor of 3.5. The blurred appearance of images b–d indicates beginning already after 2 days quite massive formation of fine particles (cf. also image c_f of Fig. SI-2). The diameter of the drop decreases during the first 3 days (from 318 to 274 μ m from image a to “c”) and then starts to increase almost explosively (from 304 to 1125 μ m from image d to f). This particular time dependence of the size of the polymerizing drops is in our understanding the most surprising results of this study and a key to shed some light in the mechanism of at least this kind of heterophase polymerization (HIEP).

The time dependence of the size of a polymerizing styrene droplet goes, for all experimental conditions studied, through a minimum which means the drop experiences first contraction followed by expansion. Figure 6 shows these two periods for the droplets depicted in Fig. SI-2.

The dotted curves in graphs a and b of Fig. 8 calculated with Eqs. 1 and 2, respectively, describe kind of theoretical limits and the comparison with the experimental data leads to important conclusions. It is necessary to point out that the diameter ratio in Eq. (1) refers to the start of the polymerization and in Eq. (2) to the minimum droplet diameter in the corresponding diameter-time curves.

First, however, looking at the experimental data for the three different recipes reveals that the presence of SDS has a much stronger influence on the change of the droplet size during both, the contraction and expansion phase, than the presence or absence of the photoinitiator. We consider this fact as proof that under both initiating condition, the reaction starts inside the droplets.

$$\frac{D_t}{D_0} = \left((1-X) + X \frac{d_m}{d_p} \right)^{1/3} \quad (1)$$

$$\frac{D_t}{D_0} = \left(\frac{1}{1-\phi_m} \right)^{1/3} \quad (2)$$

The experimental data show quite a different behavior than the curves given by Eqs. (1) and (2), particularly for the polymerization in the presence of SDS as stabilizer. Though the comparison with the experimental data is not easy because the comparison is made between two different x -axes (the independent variable is the monomer conversion (X) and the volume fraction increase (ϕ_m) in Eqs. (1) and (2), respectively, while it is the time for the experimental data) some conclusion can still be drawn. The contraction or shrinking of the droplets is not only due to the polymerization reaction. The comparison with ethyl benzene as unreactive model compound shows that a certain amount of the oil phase is transferred into the continuous water phase corresponding to its solubility at least. However, the much stronger shrinking of the drop in the presence of SDS is an experimental fact which cannot be explained alone with solubility or even solubilization by surfactants in solution [24]. The general driving force is the equilibration of the chemical potential which necessarily must be taken into account (cf. below). Interestingly, from the shrinking of polymerizing droplets alone, even if they are so large that one is tempted to assume bulk polymerization kinetics for which dilatometry is a useful kinetic tool, reliable conclusion regarding the monomer conversion is not possible.

The observed expansion of the droplets at a certain stage of polymerization (monomer conversion) appears even more mysterious than the super-shrinkage. Also here, the effect is the much stronger in the presence of SDS. The assumption that swelling with monomer contributes to this effect is quite

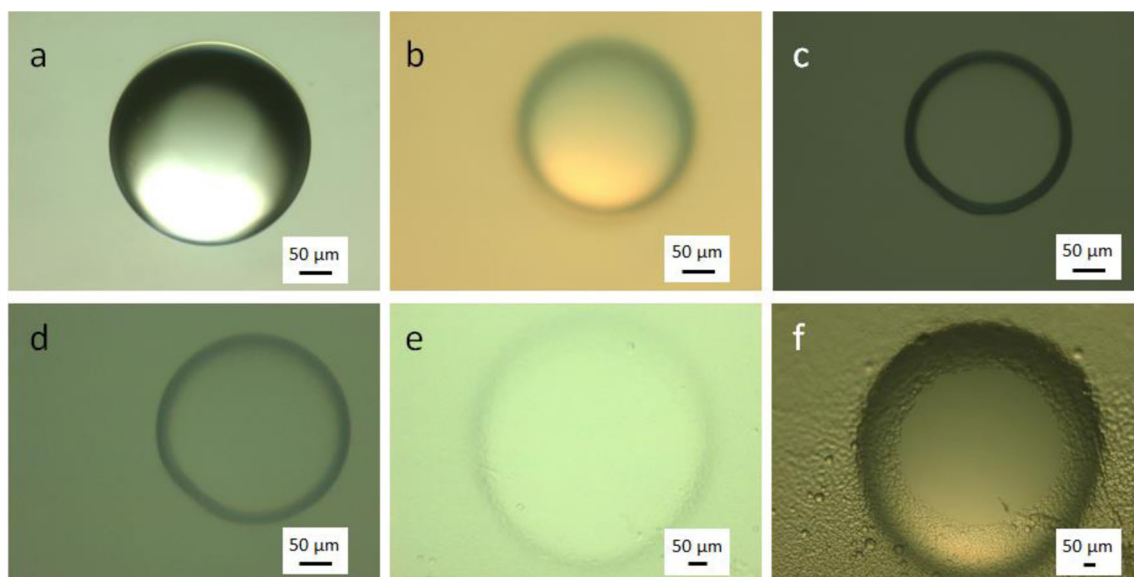


Fig. 5 Time sequence of images showing characteristic features of a polymerizing styrene droplet during surfactant-free polymerization but with photoinitiator; **a** after placing the cuvette in the holder, **b** after 48 h, **c** after 72 h, **d** after 120 h, **e** after 240 h, **f** after 458 h; the bars indicate 50 μm

reasonable because there is a monomer phase on top of the aqueous phase and the monomer conversion is surely neither there nor in all other drops the same as in the particular drop under observation. Consequently, redistribution of the monomer can happen driven by the requirement to equilibrate the chemical potential. So, swelling with monomer is possible but rather unlikely the main reason for expansion because (1) the polymerization also takes place in the bulk monomer phase, (2) the final state of the expansion leads to high ϕ_m values (greater than 0.8 or even greater than 0.9 in the presence of SDS), and (3) the enlargement is quite fast compared with the swelling of the beads (cf. above). Another argument against the assumption that swelling with monomer causes the expansion is the corona formation (cf. micrograph $b_{1,t}$ of Fig. SI-2

and micrograph f of Fig. 5) which, however, has not always been observed. Corona formation actually indicates the opposite process that is, instead of uptake the release of matter which is detected due to enhanced scattering.

For the surfactant-free polymerizations in the presence of photoinitiator, five repeats have been evaluated with respect to the polymer content in the upper monomer phase and the properties of the turbid water or latex phase. Despite the fact that the polymerization time varied between about 50 and 120 h, the solids content in the monomer phase was almost constant ($29.3 \pm 3.3\%$) with a slight tendency to increase with duration of the polymerization (from about 26 to 35%). In contrast, the solids content of the water phase is clearly below 1% but the average particle size grows exponentially with

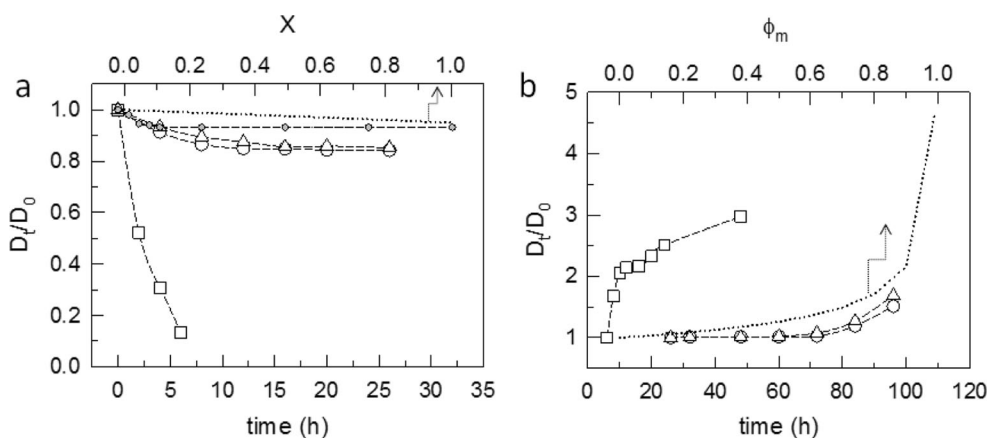


Fig. 6 Relative change of the drop diameter (D_t/D_0) during the phase of contraction (**a**) and expansion (**b**) of polymerizing styrene droplets for various polymerization conditions; *open circles* initiator- and surfactant-free polymerization, *triangles up* surfactant-free but with photoinitiator, *open squares* initiator-free but with SDS; D_0 means the initial drop diameter for each phase and D_t the diameter at given time; the dotted

line (upper x-axes) is the curve for contraction caused by only polymerization in dependence on monomer conversion, X , (cf. Eq. 1, graph **a**) and expansion for volume fraction increase, ϕ_m , (cf. Eq. 2, graph **b**); the *grey circles* in graph **a** are experimental data obtained for ethyl benzene droplets

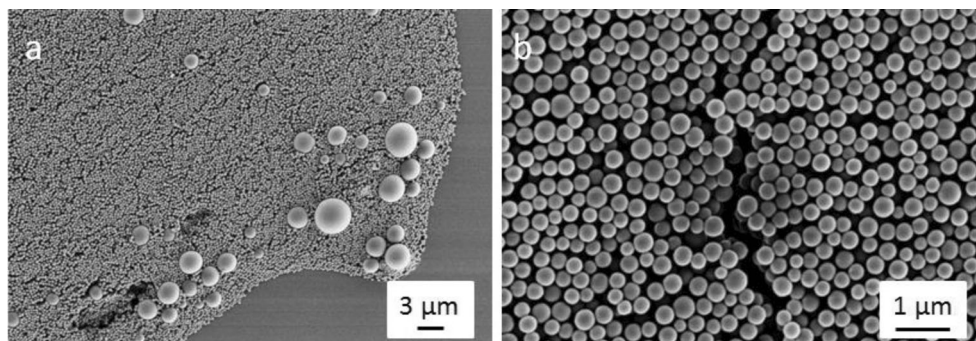
time from 380 to 710 nm. SEM images of the latex phase reveal a few particles in the size range above 5 μm but the absolute majority of the particles are in the size range below 500 nm (Fig. 7). The molecular weight of the polymer generated in the particles inside the aqueous phase is by more than a factor of ten higher than that of the polymer originating from the bulk phase.

For us, the most exciting question is how these small particles are generated and stabilized because the polymerization is carried out in the cuvette without stirring (remember, the droplets were generated just by gently shaking of the cuvette), surfactant-free, and in the presence of the superhydrophobic Irgacure 819 restricting initiation to the monomer phase.

Variation of the initiation site

The polymerization results presented so far clearly show that the size of the polymer particles (at least of the vast majority of the particles) is much smaller than that of the monomer droplets (cf. Figs. 2 and 7). This is even the case when the polymerization is started exclusively inside the monomer droplets either initiator-free via self-photoinitiation of styrene (which needs at least two styrene molecules in close contact [2]) or with the superhydrophobic Irgacure 819. Also, this effect is not changed in principle when the polymerization is carried out with or without stirring and in the presence or absence of emulsifier (SDS) or micelles. The experimental results provided strong hints that the larger drops are somehow the source for the smaller particles. This, within the common frame of mechanistic ideas of heterophase polymerizations, quite weird working hypothesis should be backed up by a series of heterophase polymerizations with poly(vinyl alcohol) as sole stabilizer and nine very different thermal initiators ranging from ionic or nonionic completely water-soluble such as ammonium peroxodisulfate or V50, to mainly or practically exclusively oil-soluble initiators such as BPO and V65, respectively. SEM micrographs showing typical features for the hydrophobic and hydrophilic initiators are put together in Figs. 8 and 9, respectively.

Fig. 7 SEM micrograph of the particles in the latex phase as generated during the surfactant-free photoinitiated styrene polymerization (cf. micrograph b_{21} of Fig. SI-2); the *bar* in micrographs **a** and **b** indicates 3 and 1 μm , respectively



Quite surprisingly, the SEM micrographs show on the one hand remarkably similar features for all initiators, regardless the very different solubility in water, but on the other hand also a distinct dependence of the results on this property of the initiators. All polymer dispersions contain particles of significantly different size (at least two distinctly different size classes), thereby the surface of the larger particles is covered by the smaller ones. The proportion of smaller particles apparently depends on the water solubility of the initiator in a way that it is larger the higher the initiators' solubility in water. The size of the smaller particles seems to depend also on the type of initiator. The size range of the latex particles is for BPO between 50 and 200 nm, for V65 between 150 and 300 nm, for VA-086 between 100 and 700 nm, for KPS between 150 and 400 nm, for V50 between 100 and 300 nm, and for V501 between 150 and 500 nm.

Notably, the morphology of the covered structures resembles that of “heterocoagulates” obtained by blending of different colloids [25, 26] for which later names such as “supraparticles” or “colloidosomes” have been coined [27, 28]. The use of emulsion droplets as templates for the assembly of preformed colloidal particles is a typical strategy to fabricate these structures [27–29].

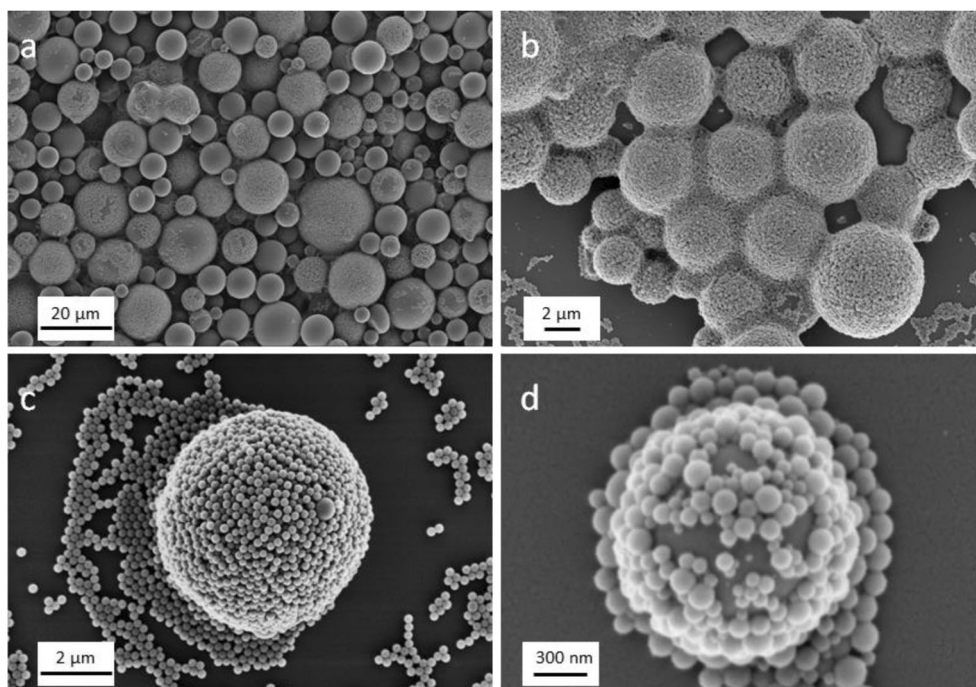
Discussion

Summary of experimental facts

Up to this point, we have presented quite diverse experimental results between which at glance only hardly a connection can be established. Before, however, trying to bring all the experimental facts together and to construct a uniform mechanistic picture, it seems to be advisable to sum up the crucial results.

1. The pressure in the reaction vial has a strong influence on the latex conversion and final particle size during HIEP. The lower the pressure is, the higher the latex conversion and the smaller the latex particle size.

Fig. 8 SEM micrographs of PS particles from heterophase polymerization with PVAI stabilizer and hydrophobic initiators V65 (micrographs **a**, **c**) and BPO (micrographs **b**, **d**); the *bar* indicates 20 μm (micrograph **a**), 2 μm (micrographs **b** and **c**), 300 nm (micrograph **d**)

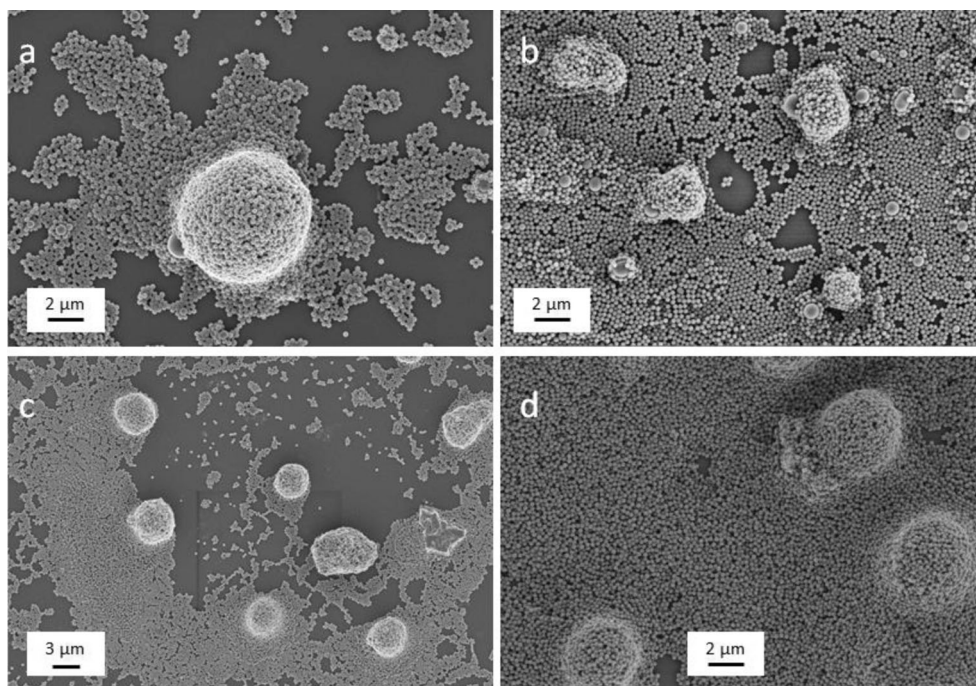


2. The uptake of solvent by PS beads is fastest for free moving beads which are in direct contact with the solvent. It is significantly slower for a non-moving bead also in direct contact with the solvent. In this case, a solvent layer wraps the bead and a solvent gradient with decreasing solvent fraction establishes towards the center of the bead. The uptake of monomer is significantly, by orders of magnitude, delayed when the PS bead is surrounded by an aqueous surfactant solution and the solvent has to

diffuse from a distant reservoir through the water phase to the bead.

3. Swelling of polystyrene seed particles with styrene monomer containing as low as 1 % of DVB cross-linker leads after seeded polymerization to core-shell particles which indicates inhomogeneous swelling.
4. The microscopic observation of single polymerizing droplets with a size in the upper μm -range reveals the release of much smaller particles/droplets which further polymerize

Fig. 9 SEM micrographs of PS particles from heterophase polymerization with PVAI stabilizer and hydrophilic initiators KPS (micrograph **a**), VA-086 (micrograph **b**), V501 (micrograph **c**), and V50 (micrograph **d**); the *bar* indicates 2 μm (micrographs **a**, **b**, **d**) and 3 μm (micrograph **c**)



and cause the formation of a common latex phase. In addition, shortly after starting the polymerization, the drop decreases in size but later, at higher conversion, the size increases again above its initial value. The increase is sometimes accompanied by corona formation or even complete disappearance of the drop (explosion). The observed effects are independent of the particular initiator and stabilizer.

- Styrene emulsion polymerization with PVAI as sole stabilizer leads to formation of particles with colloidosome-like morphology independent of the nature of the initiator. However, the proportion of the smaller and larger particles in the dispersion increases and decreases, respectively, with increasing hydrophilicity of the initiator.

Thermodynamic backup of the experimental findings

Let's consider firstly the very classical case of batch ab initio emulsion polymerization of moderately hydrophobic monomers which are solvents for their polymers with radical formation inside the droplets. An analysis of the stability of the monomer drops in the course of the polymerization, starting from the initial monomer emulsion and ending with the final polymer dispersion, is possible by means of Eq. (3) considering the chemical potential of a monomer emulsion in comparison to the bulk monomer as reference state ($\Delta\mu_m(D_d=\infty)$). Remember, $\Delta\mu$ is an expression for the "chemical force" and a powerful thermodynamic function to characterize the direction of a chemical transformation and the properties of an equilibrium state. For the following analysis, we assume that the droplets are efficiently stabilized against coagulation/coalescence by a proper surfactant or stabilizer. The main driving force for possible instability of the droplet size distribution is Ostwald ripening and its suppression contributes greatly to the stability of both the initial and polymerizing monomer emulsion.

$$\frac{\Delta\mu_m}{RT} = \frac{\mu_m(D_d) - \mu_m(D_d = \infty)}{RT} = \frac{c_1}{D_d} - x_{0p} \left(\frac{D_{0d}}{D_d}\right)^3 - c_2 x_{0p}^2 \left(\frac{D_{0d}}{D_d}\right)^6 \quad (3)$$

$$c_1 = \frac{4\sigma v_m}{RT} \quad (3a)$$

$$c_2 = c_p \frac{v_m}{RT} \quad (3b)$$

D_d is the droplet size (independent variable), D_{0d} and x_{0p} are the size and the polymer fraction at given conditions (particular independent parameters), and c_1 and c_2 are constants defined by Eq. (3a) and (3b), respectively. The swelling pressure, P_S , is a function of the polymer fraction inside the

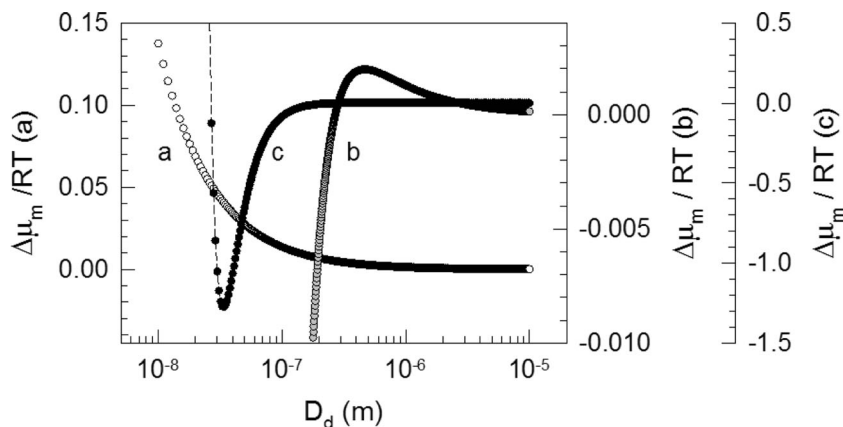
particles (x_p), and c_p is a constant resulting from fitting experimental swelling pressure data to the polymer fraction. For PS-gels swollen with chloro-benzene, the experimental PS data can be fitted with a quadratic relation $P_S = c_p x_p^2$ [30].

The first two terms on the right hand side of Eq. (3) describe the stability of emulsion droplets as discussed by Kabalnov and Webster [31–33], and the third term is the necessary consideration of a swelling pressure as discussed in [10, 11]. The concentration of monomer inside a latex particle corresponds to a situation which is known as confined swelling causing the development of a swelling pressure [34]. A latex particle behaves with respect to swelling, regardless the polymer is cross-linked or not, absolutely comparable with a polymer gel inside mechanical confinement. In the latex, the confinement is created by the interfacial tension between the particle and the continuous phase. It is important to note that the swelling pressure is the larger the lower the monomer fraction inside the particles and that the force connected with it can reach substantial values and can be used to perform real volume work [35].

The graph of Fig. 10 summarizes the contribution of each of the right hand side (rhs) terms of Eq. (3). The first rhs-term is the contribution of the Laplace pressure to the chemical potential of a pure droplet. If $x_{0p}=0$ and the $c_1>0$, this term alone describes the stability behavior of the non-polymerizing monomer emulsion. Since $\Delta\mu_m$ is for all D_d greater than zero and the first derivative with respect to D_d , $\frac{1}{RT} \frac{d\mu_m}{dD_d} = -\frac{c_1}{D_d^2}$ always negative, this situation is thermodynamically (and kinetically) unstable. If the mechanical comminution is switched off, the monomer emulsion will quickly phase separate. Now, including the second rhs-term of Eq. (3), a situation is considered quite a short period of time after initiation of the polymerization where the polymerizing droplet contains already polymer chains long enough to be insoluble in the continuous phase. For this scenario, the curve describing the dependence of $\Delta\mu/RT$ on the drop size has changed considerably showing that for certain values of D_d and x_{0p} the thermodynamic stability criteria ($\Delta\mu_m < 0$ and $\frac{1}{RT} \frac{d\mu_m}{dD_d} > 0$) are met. In addition, there is a range indicating metastability or kinetic stability ($\Delta\mu_m > 0$ and $\frac{1}{RT} \frac{d\mu_m}{dD_d} > 0$) of the monomer emulsion. It is important to emphasize that the value of x_{0p} imparting stability to a drop against Ostwald ripening depends on the drop size. It is typically larger for smaller drops. Note, in miniemulsions prepared for polymerization, x_{0p} corresponds to the concentration of the hydrophobe.

The third rhs-term considers the swelling pressure and is particularly important for higher x_{0p} values, in general corresponding to higher monomer conversion. The addition of the swelling pressure term changes the $\Delta\mu_m - D_d$ curve both qualitatively and quantitatively. The curve shows distinct regions indicating instability and stability of the monomer-polymer emulsion. Interestingly, the stability region is shifted towards lower D_d values.

Fig. 10 Correlation between the excess chemical potential ($\Delta\mu_m/RT$) and the drop size (D_d) calculated with Eq. (3) considering *a* only the first rhs-term, *b* the first and the second rhs-term, and *c* all three rhs-terms; for this set of data, $x_{op}=0.1$ and $D_{od}=100$ nm



The important result of this thermodynamic consideration is that polymer formation inside polymerizing droplets can cause increasing stability of the droplets because the polymer molecules are lyophobic. However, ongoing polymerization which leads to increasing polymer content in the polymerizing droplets shifts the start of the thermodynamically stable region (minimum in curve *c* of Fig. 10) towards lower D_d values.

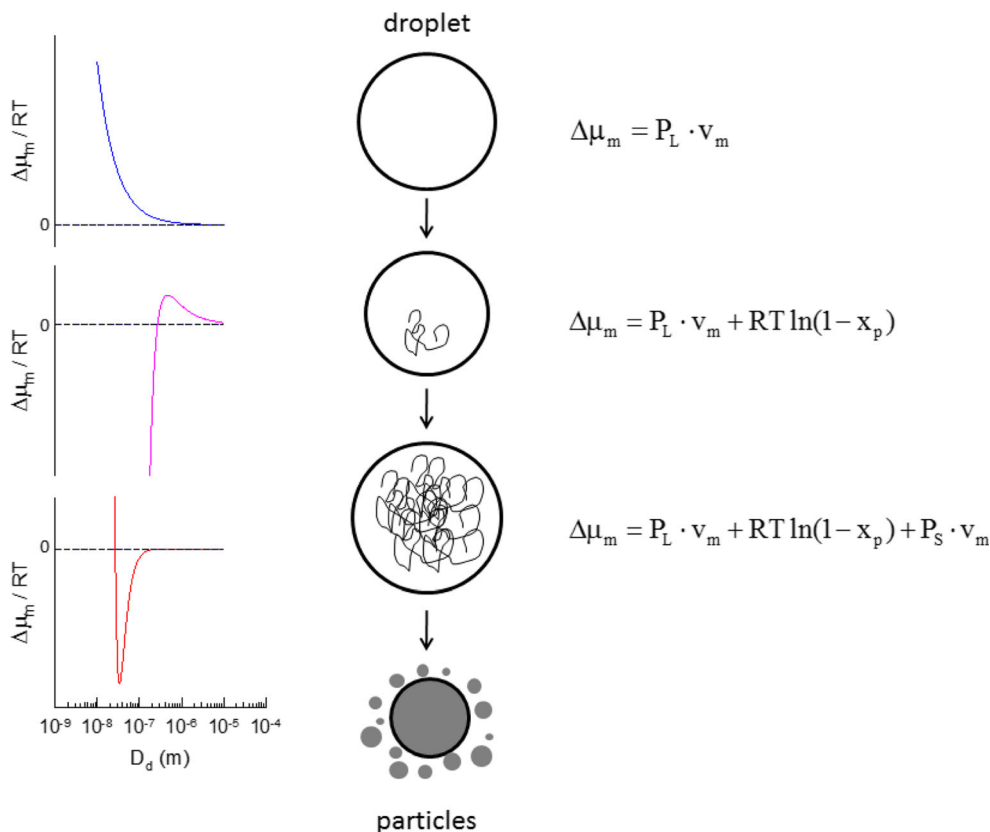
A unified mechanistic picture

The seemingly mismatched experimental data presented in the former section can, nevertheless, be combined into a unified mechanism of polymerization in monomer emulsion. Each of

the individual experimental results described is in a particular way influenced by a pressure operating in the reaction system. The action of the pressures during the different polymerizations is the common ground which allows a unified consideration. Besides the overall pressure which in a certain range can be controlled by the experimenter, the pressures dictated by the colloidal nature of the reaction system—the Laplace and the swelling pressure—are important. The importance of P_L and P_S on the changes in the course of the reaction changes primarily in dependence on the composition of the droplets. Figure 11 summarizes our findings.

The essential implications for a general mechanism of heterophase polymerization are as follows:

Fig. 11 Schematic representation of heterophase polymerization inside monomer emulsion droplets based on experimental findings; the *middle part* sketches the transition from a single monomer droplet to many polymer particles in the final dispersion; the equations on the right hand side show the contributions to the chemical potential of the droplets in the various states of the polymerization and the corresponding graphs on the left hand side illustrate the excess chemical potential in dependence on the droplet size



1. Initiating polymerization inside the monomer drops which essentially happens or can happen with any kind of initiating system (however, it happens more frequently, for higher solubility of the initiator in the monomer phase) causes a stabilization of the droplet against Ostwald ripening because the insolubility of the polymer in the aqueous phase counteracts the Laplace pressure.

2. The increasing polymer fraction inside the droplets leads to a rising swelling pressure which causes a volume increase of the particles. The swelling pressure can be so strong that tiny droplets are expelled, and hence, it is a crucial contribution to the formation of the latex particle phase. At this stage of the investigation, we have only, more or less vague, experimental hints that a conversion greater than 30 % is needed, at least for the polymerizations described in [3].

3. The fate of the expelled droplets depends strongly on the stabilizing condition (properties and concentration of the stabilizer) applied in the particular polymerization procedure.

4. Another consequence of the swelling pressure is that it counteracts homogeneous swelling. In fact, it assists at the formation of a monomer gradient in swollen polymer particles

and the formation of core-shell type particles during subsequent polymerization.

5. Quite importantly, with respect to generalization is the fact that these ideas are independent of the particular polymerization conditions (initiating and stabilizer system, temperature, stirring, etc.) as demonstrated experimentally. However, the proportion of both the small and the large particle fraction varies with the specific polymerization conditions.

6. Most importantly, with respect to a verification of the strength of the swelling pressure are the experimental observation of an exploding particle during the polymerization (cf. a1 – a3 of Fig. 12), the internal structure of the larger particles which resemble rather that of expanded polymer particles than homogeneously filled solid polymer particles (cf. b1 – b3 of Fig. 12), and the outer morphology of the final particles showing in some lucky cases perforated and/or broken shells (cf. c1 – c3 of Fig. 12).

7. Closing the circle with respect to the data of Fig. 1, the lower the pressure inside the reactor the stronger is the action of the swelling pressure.

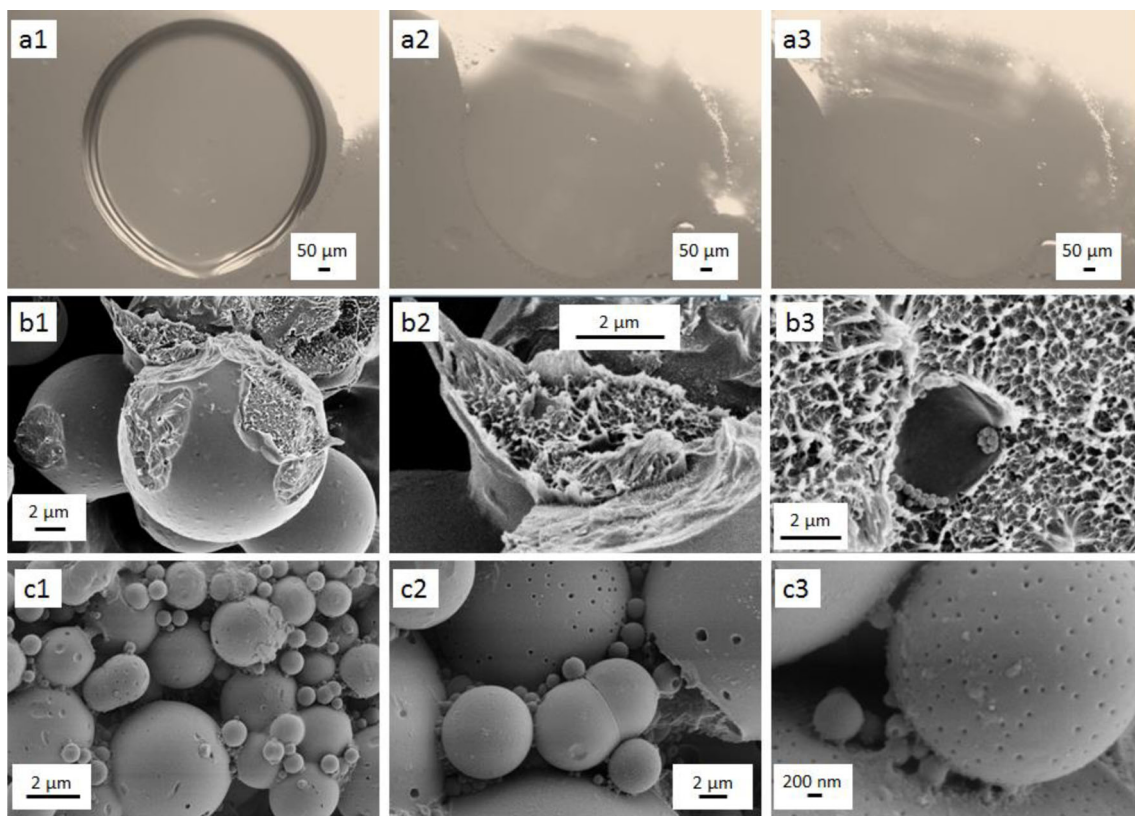


Fig. 12 Light microscopy images (*a1–a3*) and SEM micrographs (*b1–b3*, *c1–c3*) of the coagulum phase proving the strength of the swelling pressure which can cause destruction of the common solid sphere morphology; *a1*, *a2*, *a3* series of images illustrating the burst of a polymerizing droplet, the period of time between *a1–a2* and *a2–a3* is 5 and 30 min, respectively; the bars indicate 50 μm ; *b1*, *b2*, *b3* micrographs

showing the internal morphology of coagulum beads, the bars indicate for *b1*, *b2*, and *b3* 2 and 1 μm , respectively; *c1*, *c2*, *c3* series of magnification presenting perforated and broken shell-like morphology of pieces of coagulum, the bars represent 20 μm , 2 μm , and 200 nm in *c1*, *c2*, and *c3*, respectively

In this contribution, we are discussing experiments on heterophase polymerizations not in the common way of analyzing polymerization kinetics (conversion–time curves, rate of polymerization) or time-dependent changes of latex properties (particle size and particle size distribution or molecular weight and molecular weight distribution) but by studying the behavior of single droplets during polymerization, the swelling of single polymer beads, and the morphology of the coagulum. This strategy allowed us not to focus on the specific influence of recipe components, reaction conditions, and reactor design but to find out general factors influencing any kind of heterophase polymerization. The colloidal nature of the reaction system in combination with the polymer formation inside confined volumes is the most important aspect. The whole process is governed by the interaction of the overall pressure in the gas phase, the Laplace pressure in the colloidal entities, and the swelling pressure in the polymerizing droplets. This is, to the best of our knowledge, the first comprehensive discussion of the role of colloidal pressures on the course of heterophase polymerization and a new and alternate possibility to understand the process.

Acknowledgments P. T. and S. N. acknowledge a scholarship from The Thailand Research Fund (TRF) through the Royal Golden Jubilee Ph. D. Program (Grant No. PHD/0190/2553) and P.H. a fellowship and financial support within the DFG priority program SPP1420. The authors are thankful to Mrs. Rona Pitschke and Heike Runge for making all SEM micrographs.

References

- Höhne P, Krüger K, Tauer K (2013) Vapor phase composition and radical polymerization—how the gas phase influences the kinetics of heterophase polymerization. *Colloid Polym Sci* 291(3):483–500. doi:10.1007/s00396-012-2730-y
- Krüger K, Tauer K, Yagci Y, Moszner N (2011) Photoinitiated bulk and emulsion polymerization of styrene—evidence for photo-controlled radical polymerization. *Macromolecules* 44(24):9539–9549. doi:10.1021/Ma2021997
- Kim J-W, Larsen RJ, Weitz DA (2006) Synthesis of nonspherical colloidal particles with anisotropic properties. *J Am Chem Soc* 128(44):14374–14377. doi:10.1021/ja065032m
- Krüger K, Hernandez H, Tauer K (2014) Particle size-dependent effects in hydrophobically initiated emulsion polymerization. *Macromol Theor Simul* 23(3):125–135. doi:10.1002/mats.201300151
- Full Public Report (1998) Phosphine oxide, phenylbis (2,4,6-trimethylbenzoyl)- (NA/599). National Occupational Health and Safety Commission, Sydney, Australia
- Battino R, Clever HL (1966) Solubility of gases in liquids. *Chem Rev* 66(4):395
- Harkins WD (1947) A general theory of the mechanism of emulsion polymerization. *J Am Chem Soc* 69(6):1428. doi:10.1021/Ja01198a053
- van Herk A, Gilbert B (2005) Emulsion polymerisation. In: van Herk A (ed) *Chemistry and technology of emulsion polymerisation*. Blackwell Publishing Ltd, Oxford, pp 46–78
- Morton M, Kaizerman S, Altier MW (1954) Swelling of latex particles. *J Colloid Sci Imp U Tok* 9(4):300–312. doi:10.1016/0095-8522(54)90040-9
- Antonietti M, Kaspar H, Tauer K (1996) Swelling equilibrium of small polymer colloids: Influence of surface structure and a size-dependent depletion correction. *Langmuir* 12(26):6211–6217. doi:10.1021/La960159i
- Tauer K, Kaspar H, Antonietti M (2000) Equilibrium swelling of colloidal polymeric particles with water-insoluble organic solvents. *Colloid Polym Sci* 278(9):814–820. doi:10.1007/s003960000318
- Tauer K, Hernandez HF (2010) Molecular aspects of radical polymerizations—the propagation frequency. *Macromol Rapid Commun* 31(5):419–442. doi:10.1002/marc.20090060
- Kim JW, Larsen RJ, Weitz DA (2007) Uniform nonspherical colloidal particles with tunable shapes. *Adv Mater* 19(15):2005. doi:10.1002/adma.200602345
- Mock EB, De Bruyn H, Hawkett BS, Gilbert RG, Zukoski CF (2006) Synthesis of anisotropic nanoparticles by seeded emulsion polymerization. *Langmuir* 22(9):4037–4043. doi:10.1021/La060003a
- Sheu HR, Elaasser MS, Vanderhoff JW (1990) Uniform nonspherical latex-particles as model interpenetrating polymer networks. *J Polym Sci A Polym Chem* 28(3):653–667. doi:10.1002/pola.1990.080280315
- Sheu HR, Elaasser MS, Vanderhoff JW (1990) Phase-separation in polystyrene latex interpenetrating polymer networks. *J Polym Sci A Polym Chem* 28(3):629–651. doi:10.1002/pola.1990.080280314
- Skjeltorp AT, Ugelstad J, Ellingsen T (1986) Preparation of nonspherical, monodisperse polymer particles and their self-organization. *J Colloid Interface Sci* 113(2):577–582. doi:10.1016/0021-9797(86)90190-6
- Rehage G (1960) Zur Thermodynamik der Quellung. Rheinisch-Westfälischen Technischen Universität, Aachen
- Laaksonen A, Talanquer V, Oxtoby DW (1995) Nucleation—measurements, theory, and atmospheric applications. *Annu Rev Phys Chem* 46:489–524
- Lee S, Rudin A (1992) Synthesis of core shell latexes by redox initiation at ambient-temperatures. *J Polym Sci A Polym Chem* 30(10):2211–2216. doi:10.1002/pola.1992.080301016
- Thompson DW (1915) Galileo and the principle of similitude. *Nature* 95:426–427. doi:10.1038/095426a0
- Assis AKT (2004) The principle of physical proportions. *Ann Fonadtion Louis Broglie* 29(1–2):149–171
- Tolman RC (1914) The principle of similitude. *Phys Rev* 3(4):244–255. doi:10.1103/Physrev.3.244
- Klevens HB (1950) Solubilization. *Chem Rev* 47(1):1–74. doi:10.1021/cr60146a001
- Honda H, Kimura M, Honda F, Matsuno T, Koishi M (1994) Preparation of monolayer particle coated powder by the dry impact blending process utilizing mechanochemical treatment. *Colloids Surf A* 82(2):117–128. doi:10.1016/0927-7757(93)02620-T
- Kawahashi N, Matijevec E (1990) Preparation and properties of uniform coated colloidal particles. 5. Yttrium basic carbonate on polystyrene latex. *J Colloid Interface Sci* 138(2):534–542. doi:10.1016/0021-9797(90)90235-G
- Dinsmore AD, Hsu MF, Nikolaidis MG, Marquez M, Bausch AR, Weitz DA (2002) Colloidosomes: selectively permeable capsules composed of colloidal particles. *Science* 298(5595):1006–1009. doi:10.1126/science.1074868
- Velev OD, Furusawa K, Nagayama K (1996) Assembly of latex particles by using emulsion droplets as templates. 2. Ball-like and composite aggregates. *Langmuir* 12(10):2385–2391. doi:10.1021/La950679y
- Velev OD, Furusawa K, Nagayama K (1996) Assembly of latex particles by using emulsion droplets as templates. 1. Microstructured hollow spheres. *Langmuir* 12(10):2374–2384. doi:10.1021/La9506786

30. Borchard W (1966) Quellungsdruckmessungen an polystyrolgelen. Rheinisch-Westfälische Technische Hochschule, Aachen
31. Kabalnov A (2001) Ostwald ripening and related phenomena. *J Dispers Sci Technol* 22(1):1–12. doi:[10.1081/Dis-100102675](https://doi.org/10.1081/Dis-100102675)
32. Kabalnov AS, Pertzov AV, Shchukin ED (1987) Ostwald ripening in 2-component disperse phase systems—application to emulsion stability. *Colloids Surf* 24(1):19–32. doi:[10.1016/0166-6622\(87\)80258-5](https://doi.org/10.1016/0166-6622(87)80258-5)
33. Webster AJ, Cates ME (1998) Stabilization of emulsions by trapped species. *Langmuir* 14(8):2068–2079. doi:[10.1021/La9712597](https://doi.org/10.1021/La9712597)
34. Posnjak E (1912) Über den Quellungsdruck. *Kolloidchem Beih III* 12:417–454
35. Pons JL (2005) *Emerging actuator technologies: a micromechatronic approach*. John Wiley & Sons Ltd, New York